Full Length Article

Feedstock recycling of cable plastic residue via steam cracking on an industrial-scale fluidized bed

Isabel Cañete Vela [a],[*], Jelena Maric [a], Judith González-Arias [a],[b], Martin Seemann [a]

[a] *Division of Energy Technology, Chalmers University of Technology, Göteborg 412 96, Sweden*
[b] *Inorganic Chemistry Department and Materials Sciences Institute, University of Seville-CSIC, Seville, Spain*

A R T I C L E   I N F O

A B S T R A C T

The use of plastic materials in a circular way requires a technology that can treat any plastic waste and produce the same quality of product as the original. Cable plastic residue from metal recycling of electric wires is composed of cross-linked polyethene (XLPE) and PVC, which is a mixture that cannot be mechanically recycled today. Through thermochemical processes, polymer chains are broken into syngas and monomers, which can be further used in the chemical industry. However, feedstock recycling of such a mixture (XLPE, PVC) has been scarcely studied on an industrial scale. Here, the steam cracking of cable plastic was studied in an industrial fluidised bed, aiming to convert cable plastics into valuable products. Two process temperatures were tested: 730 °C and 800 °C. The results show that the products consist of 27–31 wt% ethylene and propylene, 5–16% wt. % other linear hydrocarbons, and more than 10 wt% benzene. Therefore, 40%–60% of the products are high-value chemicals that could be recovered via steam cracking of cable plastic.

1. Introduction

Plastics have become an essential part of our daily lives, with applications in packaging, infrastructure, communication, and transport. These synthetic materials are produced mostly from ethylene and propylene, which originate from fossil-based resources, producing emissions and requiring bast resources [1]. New strategies to stimulate the transition of Society towards a sustainable framework have been proposed [1–4]. These strategies should consider not only reductions in emissions of greenhouse gases (GHGs) but also the promotion of a circular economy.

In this context, promoting the circular economy entails decreasing the consumption of resources, thereby reducing dependency on fossil fuels, as well as improving waste management. The recycling of plastics, with tackles both aspects, has been growing in popularity. Polyethylene (PE) is the most frequently produced, and most often discharged, type of plastic [4–6]. Thus, most plastic waste recycling development today involves PE, albeit with a strong focus on packaging waste and pure streams, i.e., waste streams that have low levels of impurities and low contents of other plastics. Since the volumes of waste streams with these characteristics are limited, recycling rates are low. Therefore, to meet the ambitious recycling targets, there needs to be a transition from sorted plastics to more complex and challenging mixed plastic waste streams [4].

The most common recycling method for PE is mechanical recycling, i.e., re-melting, which reduces the quality of the final product. Mechanical recycling requires plastics of high purity, which means that the plastic to be recycled should be a single material (such as PE) and have low levels of impurities [7]. However, in reality, plastic waste streams contain mixtures of different types of polymers. For instance, when thermoset polymers, such as cross-linked PE (XLPE), are present in the waste blend, existing recycling methods become problematic due to the formation of permanent bonds when the thermosets are heated. Similarly, a re-melting problem arises when polyvinylchloride (PVC) or metals are part of the waste mixture [5,7,8].

One example of a mix of plastics that comprises polymer blends of PE, XLPE, and PVC is cable plastic waste. This waste is a heterogeneous mixture of thermostable polymers and thermoplastics used for jacketing electrical cables [9]. Valuable metals are mechanically separated, leaving a shredded plastic fraction [10]. However, even when advanced sorting is employed, metals, contaminants, inorganics from polymer fillers, flame retardants and/or wire leftovers remain in the plastic stream. These impurities complicate the mechanical recycling of cable plastic [11,12].

---

* Corresponding author.
E-mail address: canete@chalmers.se (I. Cañete Vela).

To tackle the challenges associated with these impurities, research has been directed towards thermochemical recycling [3,13–15]. Thermochemical recycling, which often aims to substitute the fossil-based resources used for plastics production, can be divided into two types of processes: pyrolysis and steam cracking. Pyrolysis is a thermal decomposition process that breaks down long-chain polymers into smaller molecules in an oxygen-free environment through the application of heat. In contrast, steam cracking involves the use of heat and steam. Another important distinction between the two processes lies in their respective methods for replacing fossil fuels. Currently, many plastics are manufactured using olefins such as ethylene and propylene, which are primarily derived from the steam cracking of naphtha. When plastic waste undergoes pyrolysis, it produces an oil that resembles naphtha, which can be sent to existing steam cracking facilities. Conversely, steam cracking of plastic waste can yield the desired olefins directly.

Pyrolysis is often performed within a lower temperature range, 400°–700 °C, and the dominant products are oils that can be used as alternatives to oil-based fuels, such as naphtha. There is a strong focus on using oils derived from plastic waste pyrolysis as feedstocks for steam crackers in the petrochemical industry [16–18]. However, there are problems with the contamination of heteroatoms [18]. The industrial threshold for liquid feedstocks in industrial crackers is 100 ppm for nitrogen, 500 ppm for H_2S, 3 ppm for chlorine (Cl), and 100 ppm for oxygenates [19].

Pyrolysis oils from mixed waste very often surpass these thresholds. Kusenberg et al. have reviewed more than 30 post-consumer waste pyrolysis oils, and the results showed that all pyrolysis oils exceed the Cl threshold and that many surpassed the levels for oxygen and nitrogen. For instance, vacuum pyrolysis at 500 °C, of a mixed fuel with 8% PVC, produced an oil with 12 ppm of Cl in the fraction that contained C5–C20 hydrocarbons [20]. A different process performed at 450 °C with a fuel that contained 10% PVC achieved higher concentrations of Cl in the oil, with >4,000 ppm for thermal degradation and down to about 100 ppm for a catalytic process [21]. Similar results were found for oxygen and nitrogen in the case of untreated plastic waste pyrolysis oils. These contaminants cause corrosion issues, increase coke formation, and can destroy the reactor tubes or deactivate catalysts in the separation sections of a steam cracker. Thus, those pyrolysis oils are not suitable for traditional steam cracking. Instead, decontamination or upgrading technologies are needed, such as hydro-treatment, which challenges the economic potential of plastic waste pyrolysis oil as a feedstock for steam cracking [18,22]. In other words, a mixture such as the cable plastic residues (containing PVC and XLPE) will result in complications.

In contrast, steam cracking of plastic wastes has been demonstrated to be a suitable technology for treating heterogeneous blends [16,23,24]. Based on the distribution of products, steam cracking of plastic waste can substitute for existing crackers. Naphtha cracking produces about 15%–20% fuel gas, 25% ethylene, 15% propylene, and 20% other linear hydrocarbons (HCs), by weight, with the remainder being a heavier fraction that includes aromatics. PE steam cracking at 700 °C produces about 35 wt% ethylene and 15 wt% propylene, together with about 10 wt% Benzene, Toluene and Xylene (BTX) [23]. Kaminsky et al. have shown that the steam cracking of a waste that contains 60% polyolefins and 14% PVC produces about 20 wt% ethylene, 10 wt% propylene and a similar concentration of BTX. However, the Cl content of the oil fraction was 80 ppm. Similarly, Zhou et al. have shown that during pyrolysis, for a plastic waste that contains mainly olefinic plastics and 14% PVC, 70 ppm Cl is found in the oil fraction at 700 °C [25]. However, no studies were found of such a mixture, PVC-PE, at higher temperatures [14,24,26].

Steam cracking of various plastic wastes at 700 °C has been studied extensively, and the products are similar to those obtained in a naphtha cracker [27–33]. Most of these studies were performed at a small scale in a reactor with a flow rate of a few kg/h or under. In addition, most studies focus on temperatures of 700 °C or under, and only some are found at around 800 °C, but most often using single-stream plastics such as PE. Thus, this paper focuses on the thermochemical conversion of cable plastic waste via steam cracking on an industrial scale with a waste flow rate of 100 kg/h. The fluidized bed technology has been validated for both laboratory and industrial scales [24], for solid waste that is heterogenous in size and content, as well as it is a reactor that should drive cracking reactions, which are characterised by rapid heating rates and short residence times.

The study investigates the potential for future recovery of chemicals, replacing naphtha as the feedstock needed for the production of olefins from such waste fractions. The focus is on validating the possibility to convert ash-rich cable waste (consisting of cross-linked PE and PVC) via thermochemical recycling into a useful product mixture that is suitable for the recovery of chemical feedstocks. This work aims to contribute to the deployment of thermochemical recycling at an industrial scale, while studying temperature and steam input changes. The temperatures chosen were 735 °C (to compare to the existing literature) and 800 °C. The latter is used to study the effect on the product yields for PVC-containing waste at higher temperatures, since information on steam cracking of XLPE or PVC at higher temperatures is scarce. Product yields, carbon conversion and product recovery rates were studied and compared to trials with steam cracking of pure PE, as well as naphtha steam cracking.

2. Materials and methods

2.1. Materials

The cable plastic residues used were provided by Stena Recycling and are the leftover fraction from the metal recycling of Medium and High Voltage wires. This cable residue contains around 86% dry ash-free (86%$_{daf}$) XLPE and PE, and approximately 14%$_{daf}$ chlorinated plastics (largely PVC), given the Cl content.

The cable plastic residue has a high ash content, 28% dry-weight (28%$_{dry}$), where 16%$_{dry}$ is aluminium. The aluminium is mostly metallic and can be expected to produce hydrogen when in contact with steam (following the reaction: $2Al + 6H_2O = 2Al(OH)_3 + 3H_2$). In addition, it contains a significant amount of calcium (2.6%$_{dry}$) and lower concentrations of other metals (0.31%$_{dry}$Mg and other metals at concentrations < 0.05%$_{dry}$) and a minor content of silica (0.16%$_{dry}$). The sulphur and nitrogen concentrations are low (0.02%$_{dry}$); thus, there is a low level of formation of H_2S, and NH_3 or HCN is expected. Table 1 shows the elemental composition and proximate analysis of cable plastic.

2.2. Experimental set-up

The experiments were performed in the Chalmers Research Gasification Unit (Fig. 1). The unit is composed of a Bubbling Fluidised Bed (BFB) reactor, connected to a Circulating Fluidised Bed (CFB) boiler, which provides the heat for the steam cracking in the BFB. A detailed

Table 1
Elemental analysis of cable plastic residue.

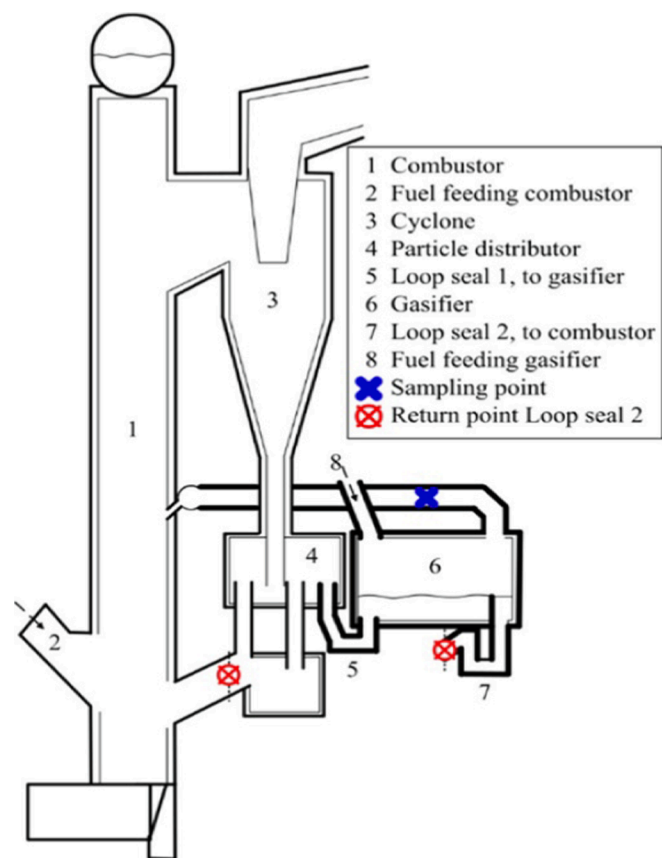|	Cable plastic
H/C ratio	1.8
Moisture (wt%)	0.7
C (%$_{daf}$)	79.2
H (%$_{daf}$)	11.8
S (%$_{daf}$)	0.03
N (%$_{daf}$)	0.03
Cl (%$_{daf}$)	8.1
Ash (%$_{dry}$)	28
O (by difference)	0.9
Volatile matter (%$_{daf}$)	96.7
Fixed Carbon (%$_{daf}$)	3.3

Fig. 1. Schematic of the Chalmers DFB steam cracker.

description of the configuration can be found elsewhere [34]. The boiler is fluidised with air and fed with wood chips and wood pellets, whereas the BFB reactor is fluidised with steam and fed with the cable plastic waste and is referred to as the steam cracker. The tests were performed at two temperatures, 735 °C and 800 °C, with steam-to-fuel ratios (SFRs) of 1.35 and 1.62. The operating conditions are listed in Table 2. The residence time of cable plastic residue in the gasifier was 4–5 min, and the gas residence time until the sampling point was approximately 10 s. The bed material used for heat transport between the reactors was silica sand.

2.3. Product sampling and measurement

Process performance was evaluated through the characterisation of the raw gas produced in the steam cracker. Two gas streams were extracted from the sampling point (blue cross in Fig. 1) and analysed after particle removal with a high-temperature filter. The first gas flow allowed the determination of the permanent gas composition and the aromatic HC content. The second gas stream was converted in a High-Temperature Reactor (HTR), at 1700 °C, cracking the HCs to form only H_2, CO, CO_2, and H_2O. Helium (20 L_N/min) was added to the process as a tracer gas, to determine the gases produced, and the measurements were made during stable operation.

In the first sampling stream, the permanent gases were analysed by

gas chromatography (GC), after quenching and removal of particles and water. A micro-GC (Varian CP4900) was employed, which was calibrated for He, H_2, CO_2, CO, CH_4, C_2H_2, C_2H_4, C_2H_6, C_3H_6, C_3H_8, O_2 and N_2. The aromatic fraction was sampled using solid-phase adsorption (SPA) [35] and analysed (four repetitions per sampled point) using GC-FID (Bruker GC-430). Thirty compounds, with boiling points intermediate to those of benzene and coronene (C_6H_6 and $C_{18}H_{22}$), were calibrated and quantified.

To characterise further the aromatic products, the non-calibrated aromatics were identified and estimated using GC–mass spectrometry (GC–MS). Table 3 provides a full list of the calibrated compounds and their categorization. Note that three nitrogen-containing compounds were calibrated, namely aniline, benzonitrile and p-toluidine, although they were not detected in any sample. For the GC–MS analysis, results with a NIST fit >80% were considered reliable, and those between 70% and 79% were considered correct [36].

In the second sampling stream, all the products were cracked into H_2, CO, CO_2, and H_2O in the HTR, the steam was condensed, and the dry gas was analysed in the micro-GC [34]. The HTR allows assessment of how much of the fuel is in the gas and establishes a carbon balance over the steam cracker. A comparison of the results from the first and second sampling streams was used to identify gaps in the species analysis.

Table 4 summarises all the measurements of the raw gas in the semi-industrial-size gasifier. The products are divided into those found in the gases and solids left in the bed. Light gases and aromatics were found in gas form. The light gases, i.e., H_2, CO, CO_2 and light HCs, were measured using the abovementioned micro-GC, excluding HCs with 4 or 5 carbons (C_4–C_5). The aromatics were assessed using the SPA method with one amine for the adsorption and using GC-FID for the analysis. The total gas was assessed with the HTR. The products that remained in the bed were unconverted or non-fully devolatilised fuel, and their levels were calculated as the difference between the fuel input and the levels measured in the HTR.

After the experiment in the industrial gasifier, the results showed high variability for the level of benzene, and significant variability of the toluene concentration. As sampling with SPA is sensitive to high concentrations in the raw gas, the completeness of the absorption of benzene and toluene was double-checked. Thus, the same conditions were reproduced in a laboratory-scale reactor, to determine whether the level of benzene was under-estimated.

The experiments were reproduced in a laboratory-scale reactor. The 9-cm-diameter reactor was operated as a BFB using nitrogen and steam as fluidising agents, to mimic the conditions in the industrial-scale reactor; a detailed description can be found elsewhere[37,38]. The reactor was operated in batch feeding mode, using 2 g of fuel fed from the top. The fluidisation was performed using 3 g/min of steam and 2 L_N/min of nitrogen, resulting in a gas residence time of 2–3 s. Two sets of experiments were conducted at the bed material temperatures of 735 °C, and 800 °C, respectively, with three repetitions of each. Helium was also

Table 2
Steam cracker operating conditions.

Name	Temp. gasifier (°C)	Steam flow (kg/h)	Fuel flow (kg$_{daf}$/h)	Steam-to-Fuel Ratio (SFR) (kg$_{steam}$/kg$_{daf}$)
735C_1.3	735	160.3	118.4	1.35
800C_1.6	800	160.6	98.6	1.62
800C_1.3	800	130.2	96.3	1.35

Table 3
Measured aromatic compounds, including calibrated and identified compounds.

Group	Aromatic compounds
Benzene	Benzene*
Toluene	Toluene*
Xylene	o-Xylene*, p-xylene*
Styrene	Styrene*, methyl-styrene*
1-ring	Other 1-ring aromatics identified by GC–MS
Naphthalenes	Naphthalene*, 1,2-dihydronaphthalene*, 1-methylnaphthalene*, 2-methylnaphthalene*
2-rings	Indene*, biphenyl* and other 2-ring aromatics identified by GC–MS
≥3-rings	Acenaphthylene*, acenaphthene*, fluorene*, phenanthrene*, anthracene*, xanthene*, fluoranthene*, pyrene*, chrysene* and other ≥ 3-ring aromatics identified by GC–MS
Oxygenated	Phenol*, o/p-cresol*, 1-naphtol*, 2-naphtol*, benzofuran*, dibenzofuran* and other oxygenated aromatics identified by GC–MS

*Calibrated compounds.

Table 4
List of compounds and the measurement techniques for the industrial- and laboratory-scale trials.

		Measurements	
	Compounds	Industrial	Laboratory
Products found in the gas	H_2, CO, CO_2 CH_4 C2–C3	GC-TCD	GC-TCD (four columns)
	C4–C5	Not measured	
	Benzene C7–C18 - 29 calibrated	SPA method using 1 SPE and analysed using GC-FID	SPA method using double SPE and analysed using GC-FID
	C7–C20 non-calibrated	SPA and identified and estimated using GC-MS	
	Soot (>C20)/ carbon deposits/ particles	Not measured	Not measured
	All the above	HTR (assess total carbon in the gas)	–
Products left in bed	Unconverted/ non-fully devolatilised fuel and other solids (>2 µm)	By difference	Post-combustion and gases analysed using GC

used as a tracing gas, and the gas was sampled using a Tedlar 0.5-L gas bag. The gas sampling time was 2 min. The aromatics were measured using the SPA method with two amines for the adsorption (instead of one in the industrial-scale reactor).

The major differences between the laboratory-scale and industrial-scale experiments were seen in the gas analysis data (Table 4). In the laboratory, an Agilent 490 micro-GC with four columns was used to analyse the light gases. He, H_2, CO_2, CO, CH_4, C_2H_2, C_2H_4, C_2H_6, C_3H_x and air were analysed with CP-Cox and PoraPLOT U columns. In addition, the detection of C_4H_x and C_5H_x HCs was carried out with a CP-Sil 5 CB column, and a CP-WAX column was used to detect benzene and toluene, to confirm that all the aromatics were successfully adsorbed to the amines. A more detailed explanation of the method can be found elsewhere [37].

In the laboratory, the carbon and hydrogen balances were established. The carbon found in the unconverted fuel was assessed by combusting the remaining product in the bed after the steam cracking of the cable plastic in the laboratory-scale reactor. Since the detection of C_4H_x and C_5H_x HCs is generic, the hydrogen calculation was based on a hydrogen-to-carbon (H/C) ratio of 2 as the average, and with values of 1.5 and 2.5 for the minimum and maximum hydrogen contents, respectively. The total hydrogen bound to Cl was estimated by assuming

that all the chlorinated HCs in the fuel (from PVC) were converted into HCl, which was equivalent to 2% of the hydrogen in the fuel.

3. Results

3.1. Gas yield distribution

This section presents the gas distributions from cable plastic steam cracking (in mol/kg$_{daf}$) for the different operating conditions. Fig. 2 displays the light gases produced during the steam cracking of cable plastic waste, at temperatures of 735 °C and 800 °C, and for two SFRs at the higher temperature. The total concentrations of light gases were 25 mol/kg$_{daf}$ at 735 °C and 32 mol/ kg$_{daf}$ at 800 °C, for both SFRs.

The most-abundant gas products were hydrogen, methane, and ethylene, for which the yields increased with increasing temperature. The hydrogen yield doubled from 4 to 8 mol/kg$_{daf}$ between 735 °C and 800 °C, while the difference between the two studied SFRs was negligible. The methane and ethylene yields increased by 30% and 15%, respectively, with the increase in temperature.

The operational temperature of 735 °C seemed to favour the formation of C_3 hydrocarbons, ethane (C_2H_6) and acetylene (C_2H_2), whereas the yields of hydrogen, methane and ethylene (H_2, CH_4, C_2H_4) were lower than at the higher temperature. Moreover, at 800 °C, the level of propane was negligible.

When it comes to oxygenated compounds, we found similar concentrations of CO_2 under the conditions studied here, with 5%–10% higher yields at the high temperature compared to the lower temperature. In contrast, the CO yield doubled with the temperature increase. The overall oxygen yield in the light gases was 5 molO/kg$_{daf}$ at 735 °C and 6.3 molO/kg$_{daf}$ under both conditions at 800 °C; in other words, the yields of CO and CO_2 were slightly different at the two SFRs studied here, although the total oxygen level in the gas was the same.

3.2. Aromatic yield distribution

Fig. 3 shows the distributions of aromatic products. Overall, a lower concentration of aromatic compounds was seen at 735 °C, i.e., 0.8 mol/kg$_{daf}$, than at higher temperatures. At 800 °C, 1.2 mol/kg$_{daf}$ was formed at the higher SFR, and slightly less, 1.1 mol/kg$_{daf}$, was formed at the lower SFR. Reducing the SFR seems to decrease slightly the formation of aromatics.

The main products in the aromatic fraction were 1-ring compounds under all three tested conditions. High concentrations of benzene were measured, although the samples displayed high variability, suggesting
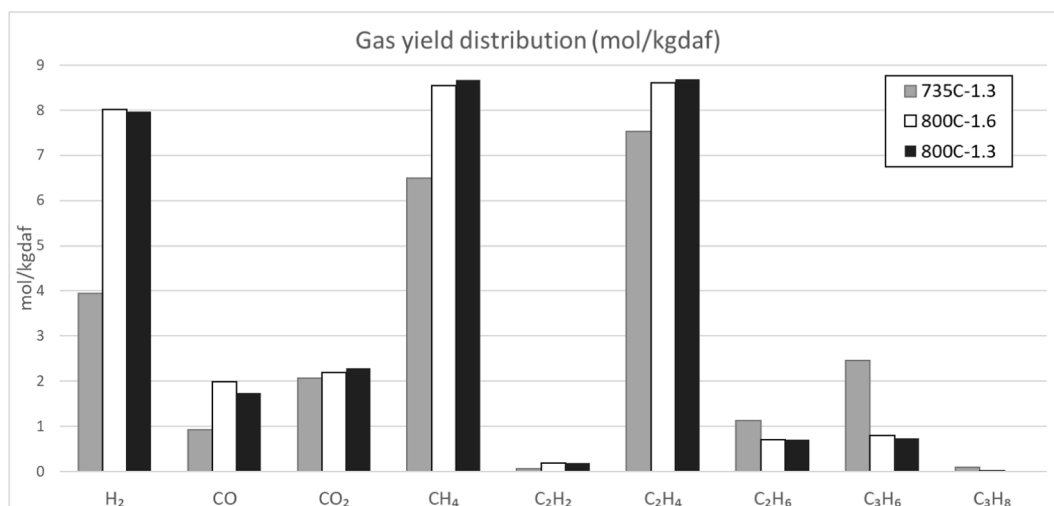

Fig. 2. *Gas yield distributions (mol/kg$_{daf}$) under the three different operating conditions (temperature–SFR).*
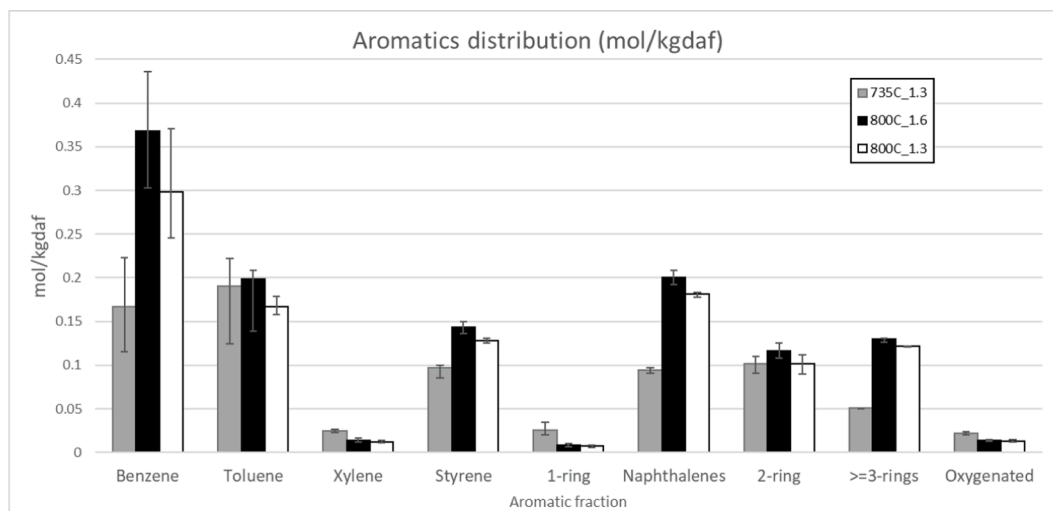
Fig. 3. Aromatics yield distributions (mol/kg$_{daf}$) under the three different operating conditions (temperature–SFR).

insufficient absorption in the SPA due to the high concentrations in the sampled gas. Similarly, the level of toluene is uncertain due to the high variability under the first two conditions.

The level of styrene increased when the temperature increased. There was also a clear increase in the levels of polyaromatic hydrocarbons (PAHs) with increasing temperature. The contents of naphthalene and $\geq$ 3-ring aromatics nearly doubled, while the levels of other 2-ring aromatics remained constant. In contrast, the levels of xylene and other 1-ring aromatics decreased with increasing temperature.

In addition, there was a decrease in the level of oxygenated compounds when the temperature increased (decreasing by almost half). Regarding other heteroatoms, some nitrogen and chlorinated compounds were detected in the GC–MS. For nitrogen, the calibrated compounds (aniline, benzonitrile and p-toluidine) were not detected, although some nitrogen-containing compounds were detected in the GC–MS. Overall, the nitrogen content of the aromatics was in all cases < 1 ppm (mg of N per kg of aromatics). The GC–MS also detected small amounts of chlorinated HCs. About 13 ppm of Cl were detected in the aromatic fraction at 800 °C in the forms of two different compounds that contained 20 and 21 carbons.

3.3. Carbon distribution

Fig. 4 shows the carbon distributions from all the experiments, with

the laboratory test results represented by dotted lines and the industrial test results indicated by solid lines. The *y*-axis indicates the percentage of carbon in each product (in mol per mol of C on a dry ash-free basis), and each product was divided per C number. The C number '0' denotes CO and CO_2. The subsequent C1–C20 compounds correspond to HCs.

The first observation that can be made is that the results from the laboratory scale and the industrial scale show the same carbon distribution. There are minor differences when it comes to CO_x, being slightly higher in the laboratory, and for PAHs, which are present at higher levels at the industrial site; the difference is more prominent at 800 °C than at the lower temperature. Moreover, the difference between the SFRs is negligible. The main differences are the C4–C5 HC fraction and benzene, as well as toluene, although the latter appears only at 735 °C. In other words, the outcome of the supplementary measurements fills the gap in the analysis of the carbon distribution in the industrial-scale experiments.

Comparing the distributions at the two studied temperatures, it is clear that there is a wider spread of the carbon distribution at low temperature, with more carbon present in the light HCs, including the C4–C5 HCs. In contrast, when increasing the temperature, or the severity, the carbons are concentrated to a greater extent in the smaller carbon HCs, mainly C1–C2, with a clear decrease in the levels of C3–C5 HCs. In addition, there is an evident increase in the PAH levels with rising temperatures, and an upwards trend in the C20 HCs.
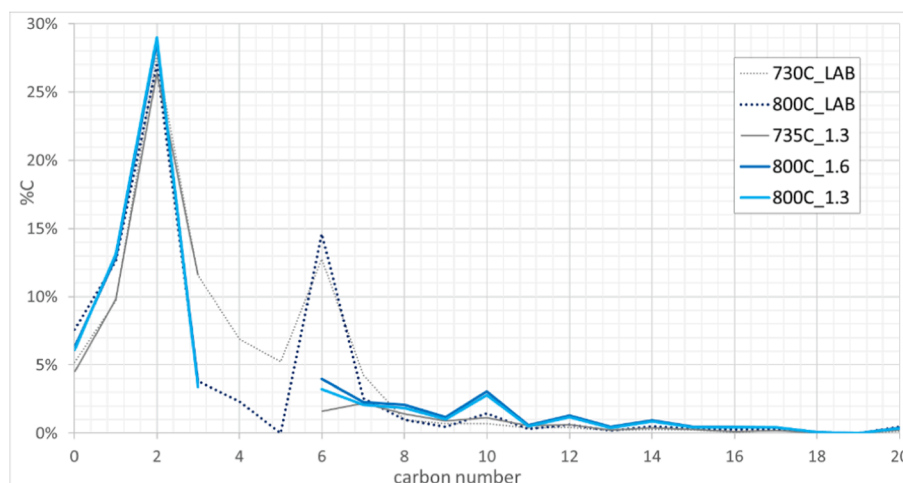

Fig. 4. Carbon distributions for all the experiments. Dotted lines, Data from laboratory-scale experiments; solid lines, data from industrial-scale experiments.

The carbon balance calculations are carried out to validate the quality of the results and to carry out a detailed assessment of the conversion of the carbon in the fuel into the different products. Table 5 shows the carbon percentages of the different measured fractions for the evaluated cases. The table depicts both the results from the industrial-scale experiments, shaded in grey, and the results from the laboratory-scale experiments. The carbon-containing products found in the gas were distributed as follows: CO and CO_2; methane; C2-C3 HCs; C4–C5 HCs; and aromatics. The aromatics were in turn divided into benzene, toluene and other 1-ring aromatics, 2-ring aromatics, and $\geq$ 3-ring aromatics.

As described in the *Methods* section, the total carbon converted into gas was measured in the HTR for the industrial tests, and by the difference in the remaining carbon in the laboratory tests. The table also displays the total known carbon, calculated by summing all the measured compounds, and the unknown carbon, which is the difference between the total converted and the known carbon. In addition, Table 5 includes the total known hydrogen and an estimate of the H/C ratio of the unknown carbon. The molar H/C ratio is calculated by assuming that all the hydrogen in the fuel is converted (i.e., subtracting the total known H% to 100%), divided by the unknown converted carbon.

Overall, the total carbon conversion in the industrial site varied substantially across the temperatures measured. At 735 °C, the overall carbon conversion was 80%C, while at a high temperature, it was around 92%C. When it comes to the different SFRs, the total carbon conversion was marginally better at the lower SFR. Not only there were minor differences in the total carbon conversion, but also the light gases. Nevertheless, the aromatic fraction was slightly larger at the higher SFR.

As observed in the carbon distribution, the carbon contents of the carbonates, methane and PAHs increased with temperature, while the carbonates increased from 4.5%C to about 6%C, methane increased from 10%C to 13%C, and the carbon contents of the PAHs doubled. In contrast, the concentrations of C2–C3 HCs decreased moderately with temperature, from 38%C to approximately 32%C. The levels of benzene and toluene seemed to increase, although this result was associated with measurement uncertainties. For other 1-ring aromatics, there was also a slight increase, due to the higher formation of styrene.

The total carbon conversion in the laboratory-scale experiments changed only slightly between the temperatures measured. At a low temperature, the overall carbon conversion was 89%C, while at 800 °C, it was around 90%C. Following the same trend as the industrial test, the carbon contents of the carbonates, methane and PAHs increased with temperature, while the carbonates increased from 5%C to about 8%C, the methane from approximately 10%C to 13%C, and the PAHs increased significantly.

Once more, the trend in the laboratory-scale experiments was the

same for the C2–C3 HCs, which moderately decreased with rising temperature, i.e., from 39%C to approximately 31%C. In the laboratory-scale experiments, the C4–C5 HCs were also measured, and showed a dramatic decrease with temperature, from 13%C to 3%C. Concerning the 1-ring aromatics, the temperature rise trend showed higher formation of benzene, from 12%C to 14%C, lower formation of toluene, from 4%C to 2%C, and slightly lower formation of other 1-ring aromatics.

As seen, temperature plays a stronger role in the yield distribution than does the steam flow. The operational temperature of 735 °C favours the formation of C3–C5 HCs, ethane (C_2H_6) and acetylene (C_2H_2), whereas the hydrogen, methane and ethylene yields (H_2, CH_4, C_2H_4) are significantly lower than at 800 °C. In other words, when increasing the temperature, the cracking severity increases, thereby producing more hydrogen, methane and ethylene.

Increasing the severity also drives poly-aromatisation. As shown in Table 5, the carbon contents of the 3-ring and higher aromatics approximately doubled with the temperature increase. The total aromatics produced were slightly higher for the high SFR. A higher SFR results in a lower residence time of the gas (about 2–3 s under the conditions studied), with the expected reduction in the aromatisation. At the same time, a higher steam flow increases the gas contacts, which may promote aromatisation. Taken together with the fact that the absorption sampling is sensitive to high concentrations of aromatics in the gas, the effect of the SFR on poly-aromatisation is inconclusive.

4. Discussion

4.1. Unknown carbon

The carbon balance from the laboratory-scale tests adds information regarding the unknown carbon at the industrial site and enhances understanding of the cable plastic product distribution. Comparing the results from the industrial site and the laboratory, it is clear that the production levels of methane and C2–C3 HCs are very similar at 735 °C. There are small differences in the levels of the carbonates, with more CO_x being formed in the laboratory compared to the industrial site. In addition, the levels of PAH formation are lower in the laboratory.

The laboratory results contribute to explaining the converted unknown, which corresponds to 18%C for the process at 735 °C on the industrial scale. The main differences are the C4–C5 hydrocarbon fraction, and the levels of benzene and toluene, due to inadequate sampling. At 735 °C, the difference between the industrial scale and laboratory scale is 25.8%C, consisting of 13%C from C4–C5 HCs and roughly 11%C from benzene and 1.8%C from toluene. While the total carbon in those species exceeds 18%C, it should be noted that the overall carbon converted in the laboratory was higher, at 89%, compared to the 80% in the

Table 5
Carbon and hydrogen balances for all the experiments.

%C	735C_1.3	735C_LAB	800C_1.6	800C_1.3	800C_LAB
CO – CO_2	4.5%	5.2%	6.3%	6.1%	7.6%
CH_4	9.8%	9.7%	12.9%	13.1%	12.6%
C2–C3	38.0%	39.3%	32.4%	32.4%	30.8%
C4–C5	n.a.	13.1%	n.a.	n.a.	2.3%
Benzene	1.5%*	12.4%	3.9%*	3.1%*	14.4%
Toluene	2.0%*	3.8%	2.3%*	2.0%*	2.3%
Other 1-ring	1.8%	1.4%	2.3%	2.2%	1.2%
Naphthalene + 2-ring	2.2%	1.6%	4.4%	4.0%	2.1%
≥3-ring	2.5%	1.7%	4.9%	4.4%	2.9%
Total converted known	*62.3%*	*89.4%*	*69.4%*	*67.3%*	*76.2%*
Converted unknown	18.0%	≈0%	22.1%	24.7%	13.7%
Total converted	**80.3%**	**88.7%**	**91.5%**	**92.0%**	**89.9%**
%H					
H_2 gas	3.4%	2.0%	7.1%	7.1%	4.3%
Total known hydrogen	79.3%	101.4%	84.9%	84.1%	85.8%
Estimated H/C for unknown	2.14	–	1.22	1.15	1.84

*high variability, under-estimated.

industrial tests. Here, the hydrogen balance can give further insight, as the unknown hydrogen is around 20%H in the industrial test, which gives a H/C ratio of 2.1 for the unknown converted fraction. This ratio suggests that these unknowns consists mostly of C4–C5 HCs, with some additional monoaromatics. This is in line with the results reported in the literature for steam cracking of PE, which yielded a similar percentage of C4–C5 HCs at temperatures in the range of 700°–750 °C [23,29,39].

Similar trends were observed for the carbon balance at 800 °C, the carbon content of methane, and the C2-C3 HCs. More CO$_x$ was formed in the laboratory, and the level of PAH formation was much lower in the laboratory than at the industrial site. In this case, the total converted carbon was very similar for both experimental scales. The main differences were reflected in the measured C4–C5 HCs, about 2%C in the laboratory, and the under-estimation of benzene, which was measured as having a 3–4-fold higher yield in the laboratory compared to the industrial-scale experiments conducted under similar conditions.

At 800 °C, the unknown carbon in the industrial site was 22–25%C. In both cases, the estimated H/C ratio was around 1.2, which is in line with the under-estimated level of benzene and the small fraction of C4–C5 HCs. Considering the carbon of the additional benzene and C4–C5 HCs, there are still about 10%C unknowns for both SFRs. From the measurements at both the laboratory and industrial scales, there are no clear indications of further missing HCs. There was, however, a clear increase in PAHs at higher severities, as shown in Figs. 3 and 4. The pronounced increase in PAHs, in terms of both molecular weight and total yield, under more-severe conditions is well-known for polyolefins, and even more so for PVC, for which a tendency towards soot is expected due to the unfavourable H/C ratio in the polymer [40,41]. Knowing the mechanism of thermal PVC decomposition, it is reasonable to suspect that a small amount of the carbon in the fuel will be found as soot, here defined as PAHs with more than 20 carbon atoms.

From the trends seen in the results from both the industrial-scale and the laboratory-scale tests, soot is a possible explanation for the missing carbon. The observed enhanced growth of PAHs with increased severity and the observed hydrogen balance strengthens this hypothesis. However, with the current setup, it is not possible to measure soot and confirm the presence of PAHs with more than 20 carbon atoms.

4.2. Steam cracking of cable plastic versus PE

As previously stated, the employed cable plastic residues consist of about 85%$_{daf}$ PE. Therefore, the cable plastic and PE steam cracking processes were compared under similar operational conditions. Table 6 shows the main products (weight) of pure PE steam cracking at 700 °C and 800 °C [23]. The cable plastic results (weight, dry-ash basis) at 735 °C and 800 °C are also presented. In addition, the main products derived from the steam cracking of naphtha are listed.

It is evident that the product distributions are similar, comprising mainly methane, olefins, and aromatics. Comparing the steam cracking of PE with that of cable plastic at around 700 °C, it is clear that the

production levels of methane, butadiene and other linear HCs are similar. However, the production levels of ethylene and propylene are significantly lower for cable plastic than for PE. In contrast, the levels of benzene and toluene formation are somewhat higher for cable plastics. This phenomenon can be attributed to lower levels of PE in the cable plastic (about 85%), as well as the presence of PVC, since dehydro-chlorination enhances the formation of monocyclic aromatics [25].

Similar observations were made when comparing the steam cracking of PE with that of cable plastic at 800 °C. However, an important difference in the product distribution was the formation of chlorinated compounds. Since PVC is present in cable plastics, HCl was produced (estimated to be about 8 wt%), which should be separated from the products. The GC–MS experiments showed small amounts of chlorinated HCs, with about 13 ppm Cl being detected in the aromatic fraction at 800 °C. While at 735 °C, the analysis was not possible, the results reported by Zhou et al. show that for a similar plastic waste, about 70 ppm Cl was found in the aromatic fraction at 700 °C, and a lower level was detected at 800 °C. Given this trend, as well as the already observed decrease in oxygenated compounds with the increase in temperature, it seems likely that the concentration of Cl at 735 °C was higher than 13 ppm.

The industrial threshold for chlorine is in the range of ppm for many equipment, and even lower concentrations are found at 800 °C, still surpassing it. However, it must be noted that the Chlorinated compounds found were aromatics that contained 20 and 21 carbons, thus, there is the possibility to separate the heavier fraction and still recover valuable chemicals such as light HCs and BTXs.

4.3. Recovery of valuable chemicals

The trend observed when increasing the temperature during PE steam cracking is similar to that seen for cable plastic steam cracking. The levels of methane and aromatics increase with temperature, while the concentrations of linear HCs decline. An important exception to this trend is ethylene, the levels of which increase with temperature for steam cracking of cable plastics.

Overall, steam cracking of cable plastic produces valuable chemicals such as ethylene and BTX. More ethylene is produced from cable plastics processed at 800 °C, and the concentrations of chlorinated and other heteroatoms are lower at that temperature; in other words, increasing the temperature enhances the recovery rates of valuable chemicals.

Moreover, if we compare the current process of steam cracking of naphtha with the steam cracking of cable plastic at 800 °C, it becomes clear that the production levels of methane and ethylene are very similar, with the main differences being observed for the C3–C5 HCs, significantly higher levels of which are produced in the naphtha process. Another difference is the production level of aromatics, in that approximately twice as much benzene is produced for steam cracking of cable plastic as compared to naphtha cracking, with similar levels of toluene, but much lower levels of xylenes.

Table 6
Main products of steam cracking (%$_{daf}$) for PE, cable plastics and naphtha.

%$_{daf}$	Steam cracking PE at 700 °C	Cable plastic at 735 °C	Steam cracking PE at 800 °C	Cable plastic at 800 °C	Steam cracking of naphtha
Methane CH$_4$	10%	10%	19%	14%	15%
Ethylene C$_2$H$_4$	36%	21%	34%	24%	25%
Propylene C$_3$H$_6$	15%	10%	1%	3%	16%
Butadiene C$_4$H$_{10}$	7%	6%*	2%	2%*	5%
Other linear HCs C2–C5	10%	10%*	4%	3%*	16%
Benzene	9%	11%*	11%	12%*	6%
Toluene	2%	3%*	1%	2%*	3%
Xylene	0.2%	0.2%	0.3%	0.1%	3%
Other aromatics	5%	5%	9%	9%	n.a.
Others**	6%	24%	19%	31%	11%

*Estimated from the results obtained at the laboratory scale.
**Refers to COx, other hydrocarbons, soot and HCl (the latter estimated to be about 8% for cable plastic).

5. Conclusions

The valorisation of cable plastic waste via steam cracking was proposed as an alternative to mechanical recycling and pyrolysis, given that cable plastic is a thermoset material and has a high content of Cl. In this study, steam cracking of cable plastic was carried out at two different temperatures and two SFRs, to evaluate the effects of these parameters on overall performance. The results indicate that the recovery of ethylene from cable plastic is comparable to that achieved using naphtha cracking.

A temperature of 800 °C seems to favour both the recovery of chemicals as well as the reduction of contaminants. Results showed that around 24 wt% ethylene and 12 wt% benzene could be recovered at 800 °C. In addition, it seems that it is likely that less Chlorinated aromatic compounds were formed but more soot was generated at this temperature. However, further research is needed to know if the chlorinated compounds hinder the recovery of the valuable chemicals as well as confirm the formation of soot and its impact to implement this technology.

CRediT authorship contribution statement

Isabel Cañete Vela: Writing – original draft, Visualization, Validation, Investigation, Formal analysis, Data curation, Conceptualization. **Jelena Maric:** Investigation, Data curation. **Judith González-Arias:** Writing – review & editing, Validation. **Martin Seemann:** Writing – review & editing, Validation, Supervision, Project administration.

Declaration of Competing Interest

The authors declare that they have no known competing financial interests or personal relationships that could have appeared to influence the work reported in this paper.

Data availability

Data will be made available on request.

Acknowledgements

References

[1] Cañete Vela I, Berdugo Vilches T, Berndes G, Johnsson F, Thunman H. Co-recycling of natural and synthetic carbon materials for a sustainable circular economy. J Clean Prod 2022;365:132674. https://doi.org/10.1016/j.jclepro.2022.132674.

[2] The New Plastics Economy: Rethinking the future of plastics & catalysing action | Shared by New Plastics Economy; n.d. https://emf.thirdlight.com/link/ftg1sxxb19tm-zgd49o/@/preview/1?o (accessed October 12, 2021).

[3] Vollmer I, Jenks MJF, Roelands MCP, White RJ, van Harmelen T, de Wild P, et al. Beyond Mechanical Recycling: Giving New Life to Plastic Waste. Angew Chem Int Ed 2020;59:15402–23. https://doi.org/10.1002/ANIE.201915651.

[4] Recycling plastics | Improving Markets for Recycled Plastics : Trends, Prospects and Policy Responses | OECD iLibrary; n.d. https://www.oecd-ilibrary.org/environment/improving-markets-for-recycled-plastics/recycling-plastics_9789264301016-7-en (accessed November 20, 2021).

[5] Hopewell J, Dvorak R, Kosior E. Plastics recycling: challenges and opportunities. Philos Trans R Soc, B 2009;364:2115. https://doi.org/10.1098/RSTB.2008.0311.

[6] Eriksen MK, Pivnenko K, Faraca G, Boldrin A, Astrup TF. Dynamic Material Flow Analysis of PET, PE, and PP Flows in Europe: Evaluation of the Potential for Circular Economy. Environ Sci Technol 2020;54:16166–75. https://doi.org/10.1021/ACS.EST.0C03435/SUPPL_FILE/ES0C03435_SI_001.PDF.

[7] Hahladakis JN, Iacovidou E. Closing the loop on plastic packaging materials: What is quality and how does it affect their circularity? Sci Total Environ 2018;630:1394–400. https://doi.org/10.1016/J.SCITOTENV.2018.02.330.

[8] Arvanitoyannis IS, Bosnea LA. Recycling of polymeric materials used for food packaging: Current status and perspectives. Food Rev Intl 2001;17:291–346. https://doi.org/10.1081/FRI-100104703.

[9] Vidales-Barriguete A, Piña-Ramírez C, Serrano-Somolinos R, del Río-Merino M, Atanes-Sánchez E. Behavior resulting from fire in plasterboard with plastic cable waste aggregates. J Build Eng 2021;40:102293. https://doi.org/10.1016/J.JOBE.2021.102293.

[10] Tange L, Drohmann D. Waste electrical and electronic equipment plastics with brominated flame retardants - From legislation to separate treatment - Thermal processes. Polym Degrad Stab 2005;88:35–40. https://doi.org/10.1016/J.POLYMDEGRADSTAB.2004.03.025.

[11] Janajreh I, Alshrah M, Zamzam S. Mechanical recycling of PVC plastic waste streams from cable industry: A case study. Sustain Cities Soc 2015;18:13–20. https://doi.org/10.1016/J.SCS.2015.05.003.

[12] Barbakadze K, Brostow W, Granowski G, Hnatchuk N, Lohse S, Osmanson AT. Separation of metal and plastic wastes from wire and cable manufacturing for effective recycling. Resour Conserv Recycl 2018;139:251–8. https://doi.org/10.1016/J.RESCONREC.2018.06.022.

[13] Ragaert K, Delva L, Van Geem K. Mechanical and chemical recycling of solid plastic waste. Waste Manag 2017;69:24–58. https://doi.org/10.1016/J.WASMAN.2017.07.044.

[14] Thunman H, Berdugo Vilches T, Seemann M, Maric J, Cañete Vela I, Pissot S, et al. Circular use of plastics-transformation of existing petrochemical clusters into thermochemical recycling plants with 100% plastics recovery. Sustain Mater Technol 2019;22:e00124. https://doi.org/10.1016/j.susmat.2019.e00124.

[15] Vela IC. Carbon materials: towards a circular economy through thermochemical recycling of mixed waste. 2022. https://research.chalmers.se/en/publication/528287.

[16] Kaminsky W, Kim JS. Pyrolysis of mixed plastics into aromatics. J Anal Appl Pyrolysis 1999;51:127–34. https://doi.org/10.1016/S0165-2370(99)00012-1.

[17] Arena U, Mastellone ML. Fluidized Bed Pyrolysis of Plastic Wastes. Feedstock Recycling and Pyrolysis of Waste Plastics: Converting Waste Plastics into Diesel and Other. Fuels 2006:435–74. https://doi.org/10.1002/0470021543.ch16.

[18] Kusenberg M, Eschenbacher A, Djokic MR, Zayoud A, Ragaert K, De Meester S, et al. Opportunities and challenges for the application of post-consumer plastic waste pyrolysis oils as steam cracker feedstocks: To decontaminate or not to decontaminate? Waste Manag 2022;138:83–115. https://doi.org/10.1016/J.WASMAN.2021.11.009.

[19] Arthur J. Baumgartner. Feedstock Contaminants in Ethylene Plants–an Update 2004. https://books.google.se/books/about/Feedstock_Contaminants_in_Ethylene_Plant.html?id=y2vzzgEACAAJ&redir_esc=y (accessed May 25, 2023).

[20] Miranda R, Pakdel H, Roy C, Vasile C. Vacuum pyrolysis of commingled plastics containing PVC II. Product analysis. Polym Degrad Stab 2001;73:47–67. https://doi.org/10.1016/S0141-3910(01)00066-0.

[21] Brebu M, Bhaskar T, Murai K, Muto A, Sakata Y, Uddin MA. Removal of nitrogen, bromine, and chlorine from PP/PE/PS/PVC/ABS–Br pyrolysis liquid products using Fe- and Ca-based catalysts. Polym Degrad Stab 2005;87:225–30. https://doi.org/10.1016/J.POLYMDEGRADSTAB.2004.08.008.

[22] Julián-Durán LM, Ortiz-Espinoza AP, El-Halwagi MM, Jiménez-Gutiérrez A. Techno-economic assessment and environmental impact of shale gas alternatives to methanol. ACS Sustain Chem Eng 2014;2:2338–44. https://doi.org/10.1021/SC500330G/ASSET/IMAGES/MEDIUM/SC-2014-00330G_0008.GIF.

[23] Kaminsky W, Schlesselmann B, Simon C. Olefins from polyolefins and mixed plastics by pyrolysis. J Anal Appl Pyrolysis 1995;32:19–27. https://doi.org/10.1016/0165-2370(94)00830-T.

[24] Scheirs J, Kaminsky W. Feedstock Recycling and Pyrolysis of Waste Plastics: Converting Waste Plastics into Diesel and Other Fuels. 2006. p. 1–785. https://doi.org/10.1002/0470021543.

[25] Zhou H, Wu C, Onwudili JA, Meng A, Zhang Y, Williams PT. Influence of process conditions on the formation of 2–4 ring polycyclic aromatic hydrocarbons from the pyrolysis of polyvinyl chloride. Fuel Process Technol 2016;144:299–304. https://doi.org/10.1016/J.FUPROC.2016.01.013.

[26] Williams PT, Williams EA. Fluidised bed pyrolysis of low density polyethylene to produce petrochemical feedstock. J Anal Appl Pyrolysis 1999;51:107–26. https://doi.org/10.1016/S0165-2370(99)00011-X.

[27] Kaminsky W, Schmidt H, Simon CM. Recycling of mixed plastics by pyrolysis in a fluidised bed. Macromol Symp 2000:191–9.

[28] Erkmen B, Ozdogan A, Ezdesir A, Celik G. Can Pyrolysis Oil Be Used as a Feedstock to Close the Gap in the Circular Economy of Polyolefins? Polymers 2023, Vol 15, Page 859 2023;15:859. https://doi.org/10.3390/polym15040859.

[29] Kaminsky W. Chemical recycling of plastics by fluidized bed pyrolysis. Fuel Commun 2021;8:100023. https://doi.org/10.1016/J.JFUECO.2021.100023.

[30] Mandviwala C, Berdugo Vilches T, Seemann M, Faust R, Thunman H. Thermochemical conversion of polyethylene in a fluidized bed: Impact of transition metal-induced oxygen transport on product distribution. J Anal Appl Pyrolysis 2022;163:105476. https://doi.org/10.1016/J.JAAP.2022.105476.

[31] Peng Y, Wang Y, Ke L, Dai L, Wu Q, Cobb K, et al. A review on catalytic pyrolysis of plastic wastes to high-value products. Energy Convers Manag 2022:254. https://doi.org/10.1016/J.ENCONMAN.2022.115243.

[32] Maqsood T, Dai J, Zhang Y, Guang M, Li B. Pyrolysis of plastic species: A review of resources and products. J Anal Appl Pyrolysis 2021;159. https://doi.org/10.1016/J.JAAP.2021.105295.

[33] Miskolczi N, Bartha L, Angyal A. Pyrolysis of Polyvinyl Chloride (PVC)-Containing Mixed Plastic Wastes for Recovery of Hydrocarbons n.d. https://doi.org/10.1021/ef8011245.

[34] Larsson A, Seemann M, Neves D, Thunman H. Evaluation of performance of industrial-scale dual fluidized bed gasifiers using the chalmers 2–4-MWth gasifier. Energy Fuel 2013;27:6665–80. https://doi.org/10.1021/EF400981J/SUPPL_FILE/EF400981J_SI_001.PDF.

[35] Israelsson M, Seemann M, Thunman H. Assessment of the Solid-Phase Adsorption Method for Sampling Biomass-Derived Tar in Industrial Environments. Energy Fuel 2013;27:7569–78. https://doi.org/10.1021/EF401893J.

[36] An Integrated Method for Spectrum Extraction and Compound Identification from GC/MS Data. https://doi.org/10.1016/S1044-0305(99)00047-1.

[37] Mandviwala C, González-Arias J, Seemann Martin, Berdugo Vilches T, Thunman H. Fluidized bed steam cracking of rapeseed oil: exploring the direct production of the molecular building blocks for the plastics industry. Biomass Convers Biorefin n.d. 2022;1:3. https://doi.org/10.1007/s13399-022-02925-z.

[38] Li S, Cañete Vela I, Järvinen M, Seemann M. Polyethylene terephthalate (PET) recycling via steam gasification – The effect of operating conditions on gas and tar composition. Waste Manag 2021;130:117–26. https://doi.org/10.1016/J.WASMAN.2021.05.023.

[39] Simon CM, Kaminsky W, Schlesselmann B. Pyrolysis of polyolefins with steam to yield olefins. J Anal Appl Pyrolysis 1996;38:75–87. https://doi.org/10.1016/S0165-2370(96)00950-3.

[40] Ma S, Lu J, Gao J. Study of the Low Temperature Pyrolysis of. PVC 2002. https://doi.org/10.1021/ef0101053.

[41] Yu J, Sun L, Ma C, Qiao Y, Yao H. Thermal degradation of PVC: A review. Waste Manag 2016;48:300–14. https://doi.org/10.1016/J.WASMAN.2015.11.041.